School of Medicine
TEMPLE UNIVERSITY

Personalized medicine guided synthetic lethality eliminates leukemia stem cells

Tomasz Skorski, MD, PhD, DSc
Department of Microbiology and Immunology
Fels Institute for Cancer Research & Molecular Biology
Temple University School of Medicine
Philadelphia, PA, USA

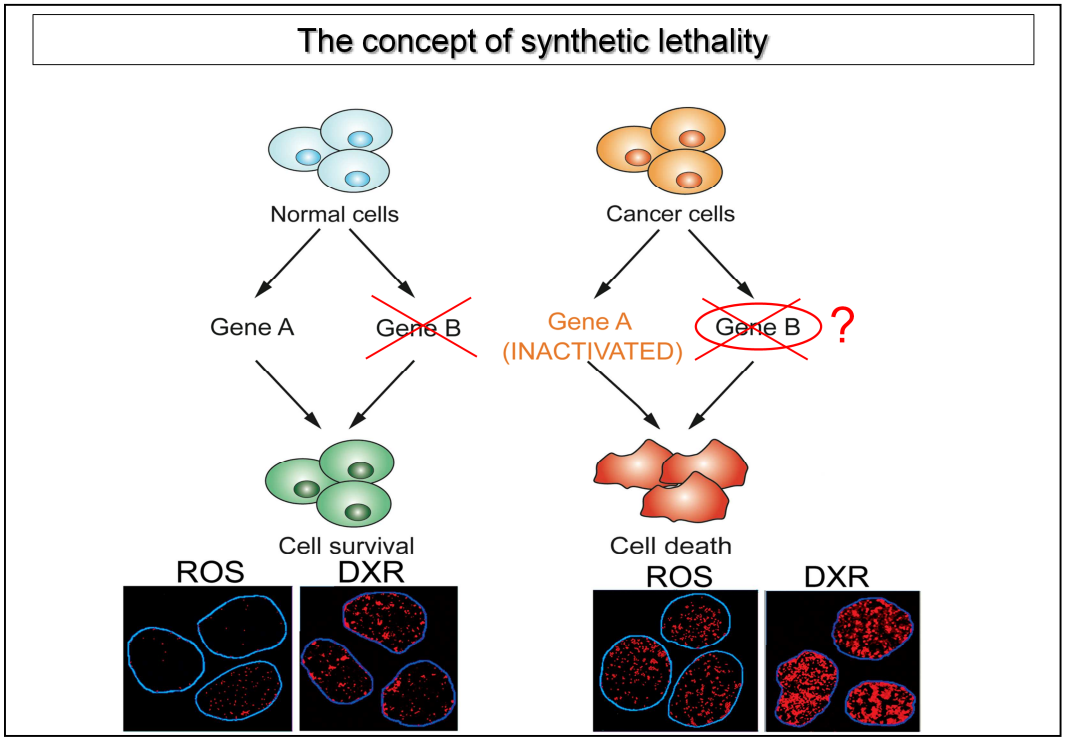

Synthetic lethality occurs when mutations affecting genes in two pathways involved in regulating a single cellular process results in cell death. In normal cells, mutation of each gene singly has no effect, since the redundant pathway is functional. In cancer cells, when one of these genes is not functional due to a cancer-relevant mutation, targeting the 2nd gene leads to cell death since both pathways are not operating properly.

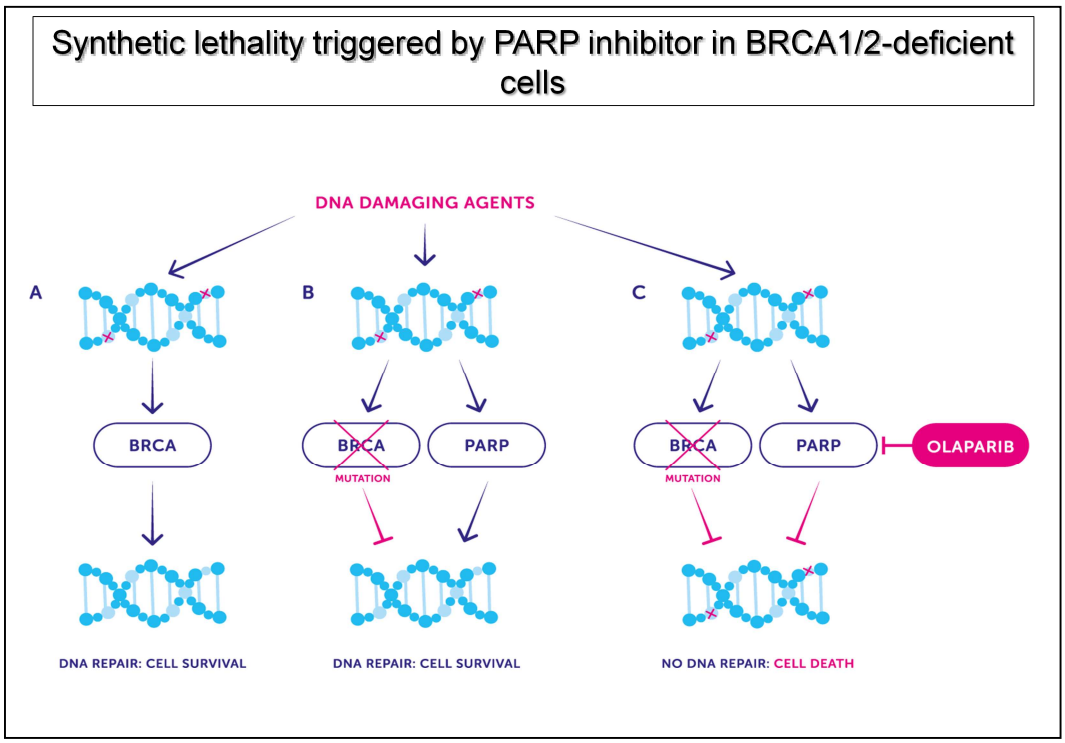

PARP1 inhibitors exerted therapeutic effect against BRCA and/or DNA-PK –deficient positive AML and ALL primary leukemia xenografts. (**A**) Microarray detection of mRNA for the indicated genes in primary AMLs (top graph) and ALLs (middle and bottom graphs) xenografts. Each circle represents individual patient: blue, gray and red circles indicate lower than average, average and higher than average expression levels in BRCA/DNA-PK -deficient AML (top graph), BRCA-deficient ALL (middle graph) and BRCA/DNA-PK – proficient ALL (bottom panel) xenograft cells. (**B**) Number of cells from individual primary xenognaft samples treated with DNR, BMN673, and DNR + BMN673; *$p<0.05$ in comparison to all other groups. (**C**, D) NSG mice (6 mice/group) were injected with 1 x 10^6 primary leukemia xenograft cells and treated with diluents (C), doxorubicin + cytarabine (DA), BMN673, and DA + BMN673. (**C**) Mean ± SD percentage of human $CD45^+$ cells in peripheral blood leukocytes; *$p<0.001$ in comparison to other groups. Representatives of flow cytometry detecting human $CD45^+$ leukemia cells (red dots) and mouse peripheral blood leukocytes (black dots) 1 week after treatment. (**D**) Median survival time ± SD; *$p<0.001$ and **$p<0.002$ in comparison to DA.

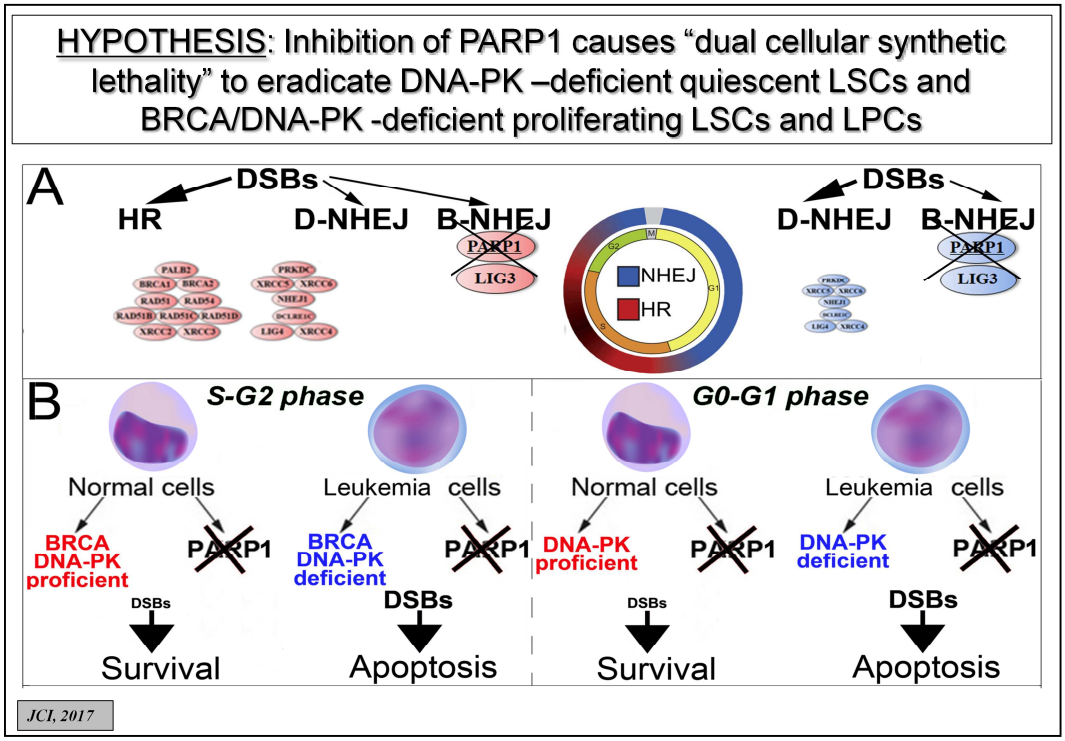

Patients with acute leukemia display a wide range of BRCA1 and 2 expression based on microarray. For further studies we chose patients with high BRCA1 and 2, symbolized by red dots, and low BRCA1 and 2 symbolized by blue dots. We validated high and low levels of BRCA1 in proliferating leukemia cells. The aptamer exerted anti-leukemia activity in brca1/2 low patients but not in brca1/2 high patients either alone or in combination with daunarubicin.

HYPOTHESIS: Inhibition of PARP1 causes "dual cellular synthetic lethality" to eradicate DNA-PK –deficient quiescent LSCs and BRCA/DNA-PK -deficient proliferating LSCs and LPCs

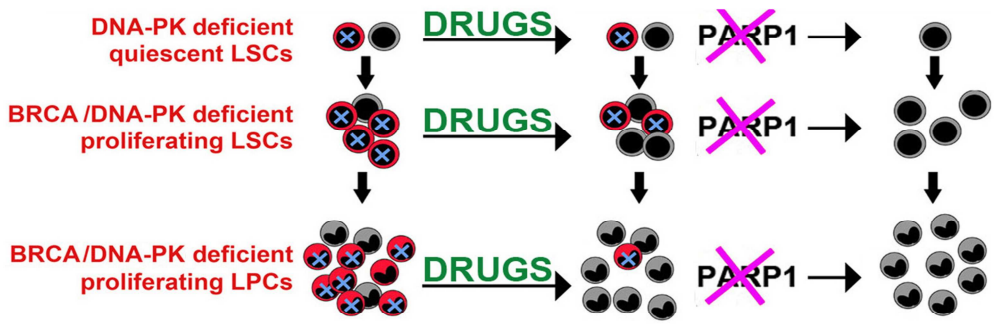

Double strand breaks are extremely lethal and if not repaired even a single unrepaired double strand break can lead to cell death. CML cells deal with increased amounts of these breaks by stimulating the major DNA repair pathways, homologous recombination and non homologous end joining. There are small amounts of DNA damage in normal cells. In CML cells however, the amount of DNA damage is much higher.

TCGA analysis identifies individual AMLs potentially displaying BRCA/DNA-PK deficiency

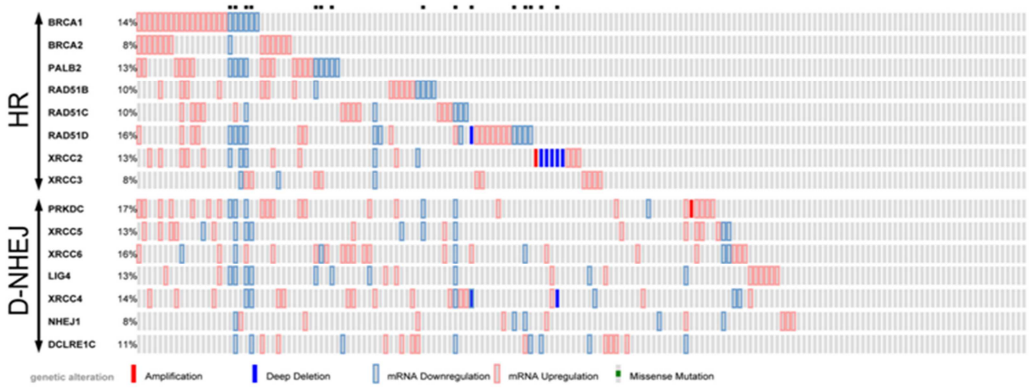

JCI, 2017

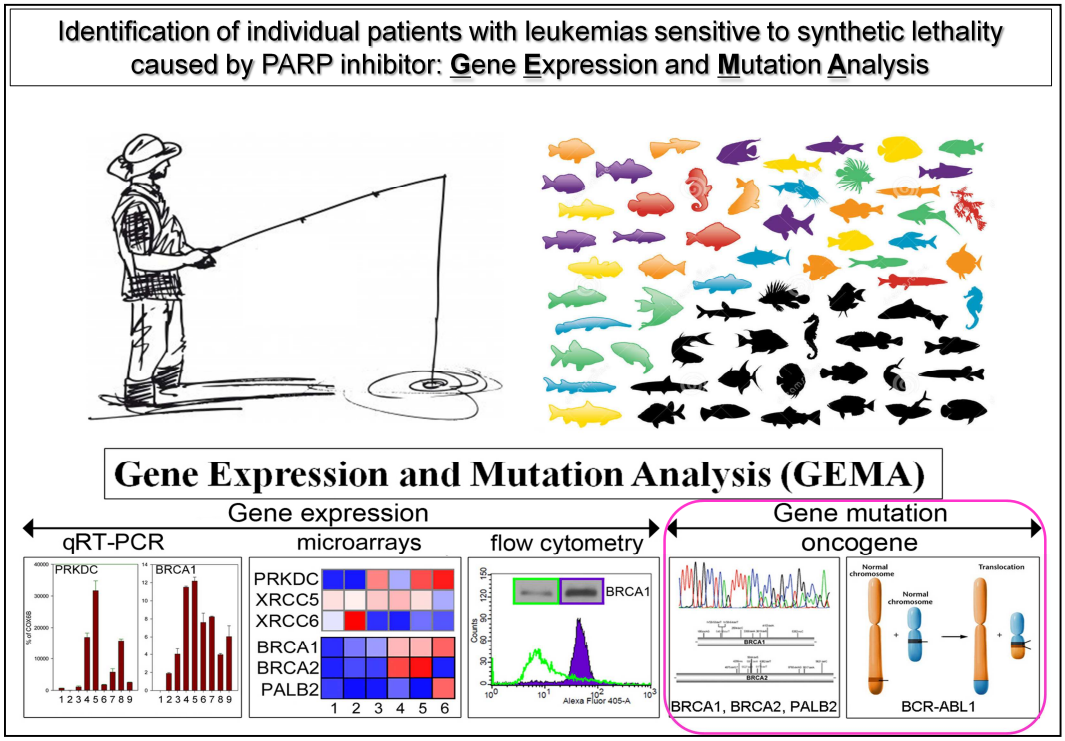

GEMA to select "BRCA-deficient" AML/ALL patients. Gene expression analysis by quantization of the expression patterns of BRCA-pathway genes by qRT-PCR, mRNA microarrays and flow cytometry. Mutation analysis by detection of particular genetic aberration (mutation, chromosomal translocation).

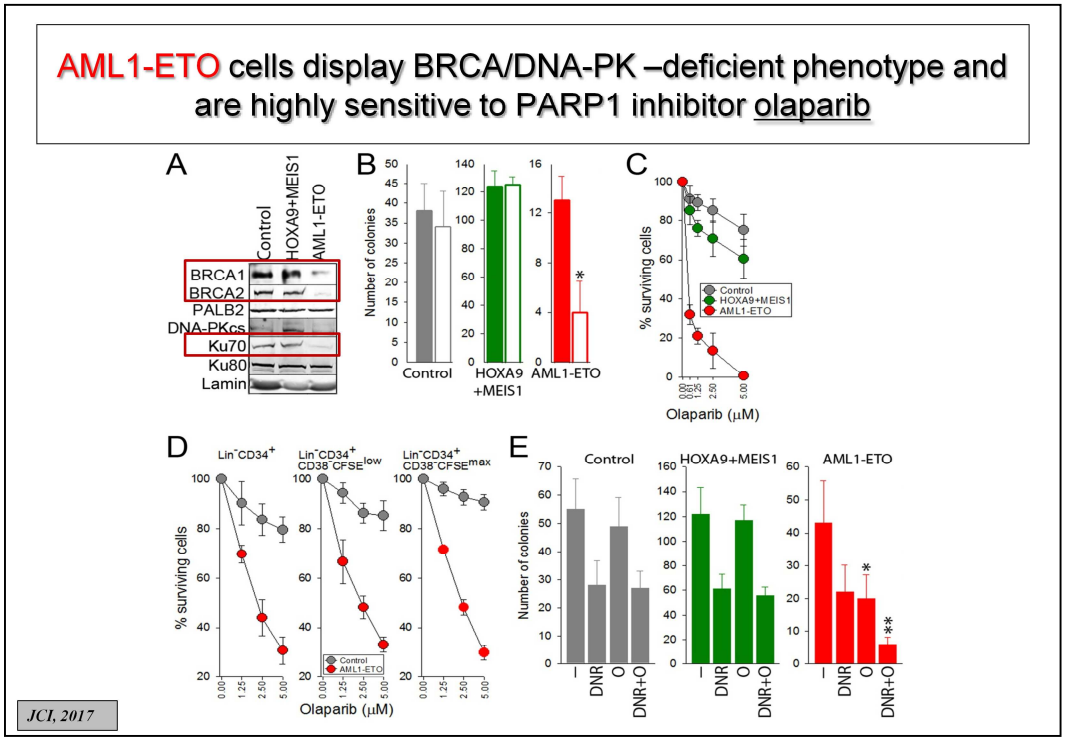

Gene Mutation profiling identified "DNA-PK and BRCA deficient" leukemias. (**A-C**) Non-transformed (Normal) murine bone marrow cells and these expressing MLL-AF9, AML1-ETO, HOXA9+MEIS1 were examined. (**A**) Western analysis, (**B**) clonogenic assay in the presence [+/+, filled bars] or absence [-/-, transparent bars] of Parp1, and (**C**) sensitivity to olaparib. (**D-E**) Olaparib (1.25 mM) eliminated $Lin^{-}CD34^{+}CD38^{-}CFSE^{max}$ quiescent LSCs and proliferating $Lin^{-}CD34^{+}CD38^{+}$ LSCs and $Lin^{-}CD34^{+}$ LPCs from (**D**) MLL-AF9 and (**E**) AML1-ETO AML patients cells (n=3 for each translocation).

BCR-ABL1 –positive cells display BRCA/DNA-PK –deficient phenotype and are highly sensitive to PARP1 inhibitor olaparib

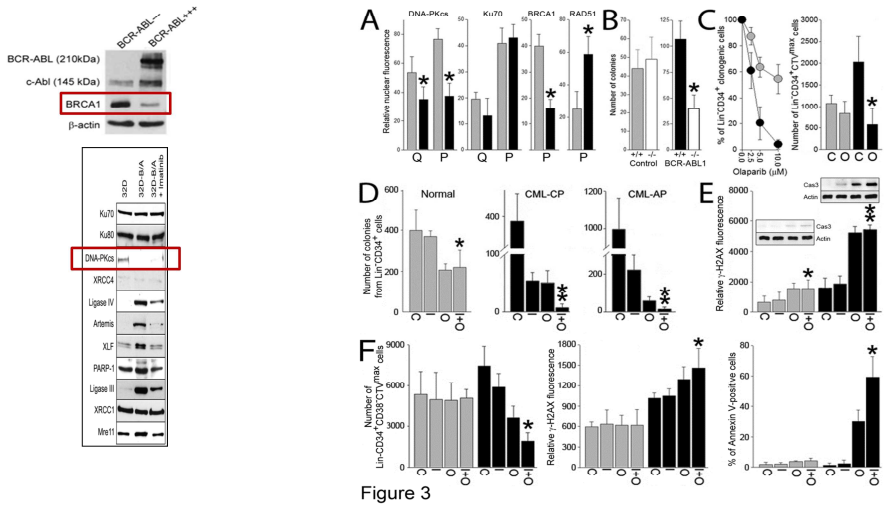

Figure 3

JCI, 2017

Gene Mutation profiling identified "DNA-PK and BRCA deficient" leukemias. (**A-C**) Non-transformed (Normal) murine bone marrow cells and these expressing MLL-AF9, AML1-ETO, HOXA9+MEIS1 were examined. (**A**) Western analysis, (**B**) clonogenic assay in the presence [+/+, filled bars] or absence [-/-, transparent bars] of Parp1, and (**C**) sensitivity to olaparib. (**D-E**) Olaparib (1.25 mM) eliminated $Lin^-CD34^+CD38^-CFSE^{max}$ quiescent LSCs and proliferating $Lin^-CD34^+CD38^+$ LSCs and Lin^-CD34^+ LPCs from (**D**) MLL-AF9 and (**E**) AML1-ETO AML patients cells (n=3 for each translocation).

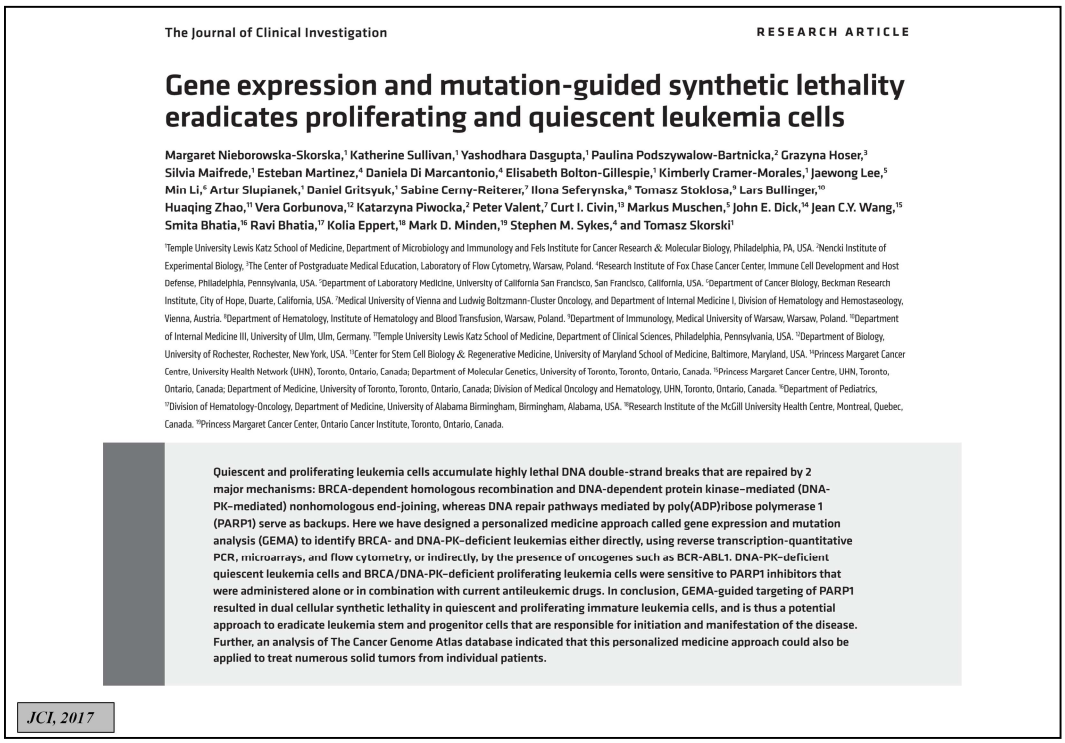

The Journal of Clinical Investigation RESEARCH ARTICLE

Gene expression and mutation-guided synthetic lethality eradicates proliferating and quiescent leukemia cells

Margaret Nieborowska-Skorska,[1] Katherine Sullivan,[1] Yashodhara Dasgupta,[1] Paulina Podszywalow-Bartnicka,[2] Grazyna Hoser,[3] Silvia Maifrede,[1] Esteban Martinez,[4] Daniela Di Marcantonio,[4] Elisabeth Bolton-Gillespie,[1] Kimberly Cramer-Morales,[1] Jaewong Lee,[5] Min Li,[6] Artur Slupianek,[1] Daniel Gritsyuk,[1] Sabine Cerny-Reiterer,[7] Ilona Seferynska,[8] Tomasz Stoklosa,[9] Lars Bullinger,[10] Huaqing Zhao,[11] Vera Gorbunova,[12] Katarzyna Piwocka,[2] Peter Valent,[7] Curt I. Civin,[13] Markus Muschen,[5] John E. Dick,[14] Jean C.Y. Wang,[15] Smita Bhatia,[16] Ravi Bhatia,[17] Kolia Eppert,[18] Mark D. Minden,[19] Stephen M. Sykes,[4] and Tomasz Skorski[1]

[1]Temple University Lewis Katz School of Medicine, Department of Microbiology and Immunology and Fels Institute for Cancer Research & Molecular Biology, Philadelphia, PA, USA. [2]Nencki Institute of Experimental Biology, [3]The Center of Postgraduate Medical Education, Laboratory of Flow Cytometry, Warsaw, Poland. [4]Research Institute of Fox Chase Cancer Center, Immune Cell Development and Host Defense, Philadelphia, Pennsylvania, USA. [5]Department of Laboratory Medicine, University of California San Francisco, San Francisco, California, USA. [6]Department of Cancer Biology, Beckman Research Institute, City of Hope, Duarte, California, USA. [7]Medical University of Vienna and Ludwig Boltzmann-Cluster Oncology, and Department of Internal Medicine I, Division of Hematology and Hemostaseology, Vienna, Austria. [8]Department of Hematology, Institute of Hematology and Blood Transfusion, Warsaw, Poland. [9]Department of Immunology, Medical University of Warsaw, Warsaw, Poland. [10]Department of Internal Medicine III, University of Ulm, Ulm, Germany. [11]Temple University Lewis Katz School of Medicine, Department of Clinical Sciences, Philadelphia, Pennsylvania, USA. [12]Department of Biology, University of Rochester, Rochester, New York, USA. [13]Center for Stem Cell Biology & Regenerative Medicine, University of Maryland School of Medicine, Baltimore, Maryland, USA. [14]Princess Margaret Cancer Centre, University Health Network (UHN), Toronto, Ontario, Canada; Department of Molecular Genetics, University of Toronto, Toronto, Ontario, Canada. [15]Princess Margaret Cancer Centre, UHN, Toronto, Ontario, Canada; Department of Medicine, University of Toronto, Toronto, Ontario, Canada; Division of Medical Oncology and Hematology, UHN, Toronto, Ontario, Canada. [16]Department of Pediatrics, [17]Division of Hematology-Oncology, Department of Medicine, University of Alabama Birmingham, Birmingham, Alabama, USA. [18]Research Institute of the McGill University Health Centre, Montreal, Quebec, Canada. [19]Princess Margaret Cancer Center, Ontario Cancer Institute, Toronto, Ontario, Canada.

Quiescent and proliferating leukemia cells accumulate highly lethal DNA double-strand breaks that are repaired by 2 major mechanisms: BRCA-dependent homologous recombination and DNA-dependent protein kinase–mediated (DNA-PK–mediated) nonhomologous end-joining, whereas DNA repair pathways mediated by poly(ADP)ribose polymerase 1 (PARP1) serve as backups. Here we have designed a personalized medicine approach called gene expression and mutation analysis (GEMA) to identify BRCA- and DNA-PK–deficient leukemias either directly, using reverse transcription-quantitative PCR, microarrays, and flow cytometry, or indirectly, by the presence of oncogenes such as BCR-ABL1. DNA-PK–deficient quiescent leukemia cells and BRCA/DNA-PK–deficient proliferating leukemia cells were sensitive to PARP1 inhibitors that were administered alone or in combination with current antileukemic drugs. In conclusion, GEMA-guided targeting of PARP1 resulted in dual cellular synthetic lethality in quiescent and proliferating immature leukemia cells, and is thus a potential approach to eradicate leukemia stem and progenitor cells that are responsible for initiation and manifestation of the disease. Further, an analysis of The Cancer Genome Atlas database indicated that this personalized medicine approach could also be applied to treat numerous solid tumors from individual patients.

JCI, 2017

PARP1 inhibitors exerted therapeutic effect against BRCA and/or DNA-PK –deficient positive AML and ALL primary leukemia xenografts. (**A**) Microarray detection of mRNA for the indicated genes in primary AMLs (top graph) and ALLs (middle and bottom graphs) xenografts. Each circle represents individual patient: blue, gray and red circles indicate lower than average, average and higher than average expression levels in BRCA/DNA-PK -deficient AML (top graph), BRCA-deficient ALL (middle graph) and BRCA/DNA-PK – proficient ALL (bottom panel) xenograft cells. (**B**) Number of cells from individual primary xenognaft samples treated with DNR, BMN673, and DNR + BMN673; *$p<0.05$ in comparison to all other groups. (**C**, D) NSG mice (6 mice/group) were injected with 1 x 10^6 primary leukemia xenograft cells and treated with diluents (C), doxorubicin + cytarabine (DA), BMN673, and DA + BMN673. (**C**) Mean ± SD percentage of human $CD45^+$ cells in peripheral blood leukocytes; *$p<0.001$ in comparison to other groups. Representatives of flow cytometry detecting human $CD45^+$ leukemia cells (red dots) and mouse peripheral blood leukocytes (black dots) 1 week after treatment. (**D**) Median survival time ± SD; *$p<0.001$ and **$p<0.002$ in comparison to DA.

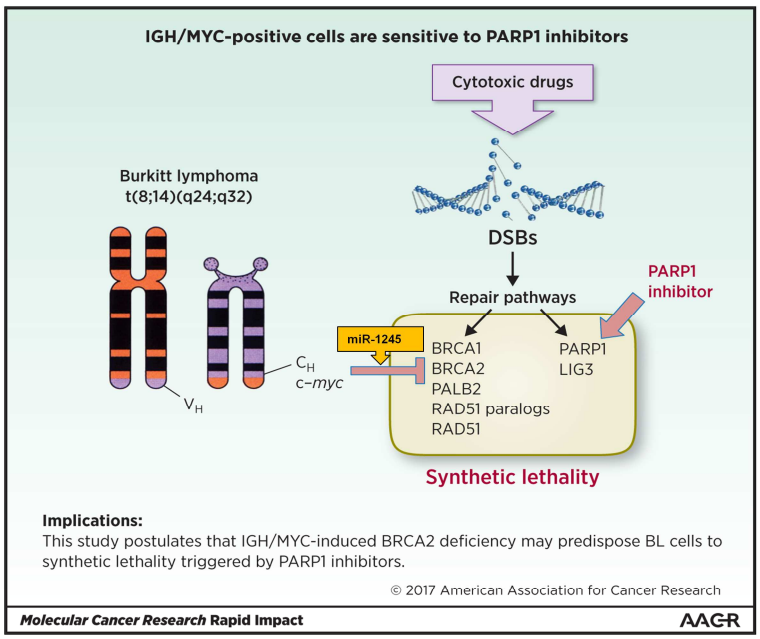
IGH/MYC-positive cells are sensitive to PARP1 inhibitors
Cytotoxic drugs
Burkitt lymphoma
t(8;14)(q24;q32)
DSBs
Repair pathways
PARP1
inhibitor
miR-1245
BRCA1
BRCA2
PALB2
RAD51 paralogs
RAD51
PARP1
LIG3
C_H
c–*myc*
V_H
Synthetic lethality
Implications:
This study postulates that IGH/MYC-induced BRCA2 deficiency may predispose BL cells to synthetic lethality triggered by PARP1 inhibitors.
© 2017 American Association for Cancer Research
Molecular Cancer Research Rapid Impact
AACR

MCR, 2017

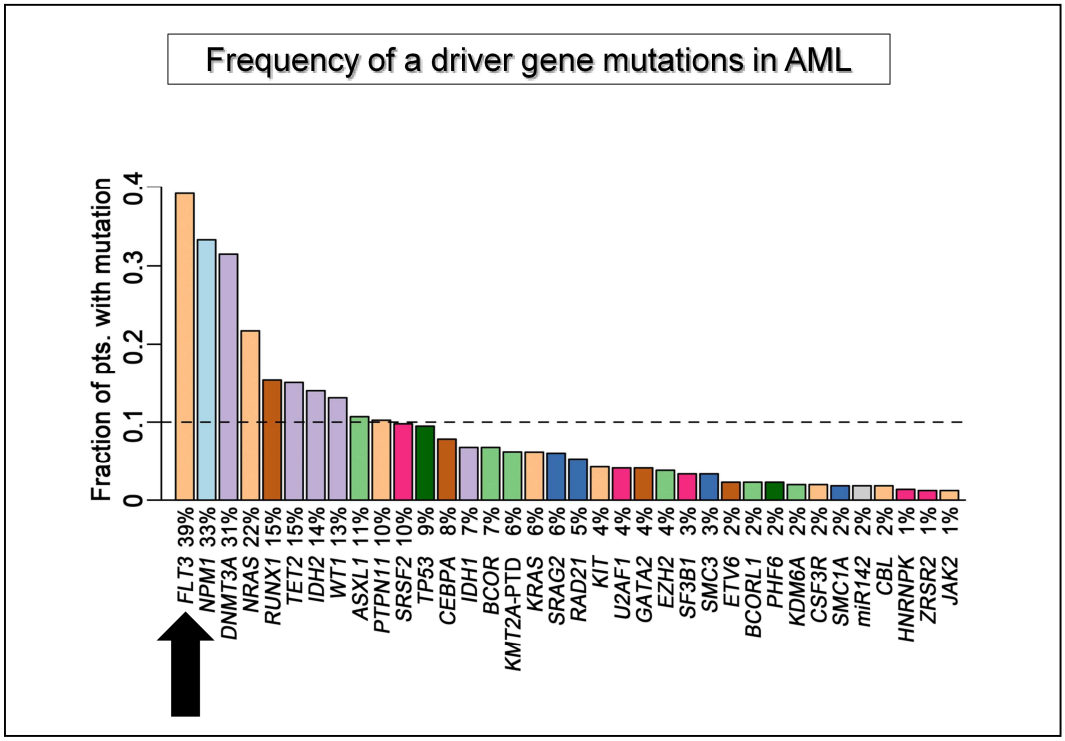

PARP1 inhibitors exerted therapeutic effect against BRCA and/or DNA-PK –deficient positive AML and ALL primary leukemia xenografts. (**A**) Microarray detection of mRNA for the indicated genes in primary AMLs (top graph) and ALLs (middle and bottom graphs) xenografts. Each circle represents individual patient: blue, gray and red circles indicate lower than average, average and higher than average expression levels in BRCA/DNA-PK -deficient AML (top graph), BRCA-deficient ALL (middle graph) and BRCA/DNA-PK – proficient ALL (bottom panel) xenograft cells. (**B**) Number of cells from individual primary xenognaft samples treated with DNR, BMN673, and DNR + BMN673; *p<0.05 in comparison to all other groups. (**C**, D) NSG mice (6 mice/group) were injected with 1 x 10^6 primary leukemia xenograft cells and treated with diluents (C), doxorubicin + cytarabine (DA), BMN673, and DA + BMN673. (**C**) Mean ± SD percentage of human $CD45^+$ cells in peripheral blood leukocytes; *p<0.001 in comparison to other groups. Representatives of flow cytometry detecting human $CD45^+$ leukemia cells (red dots) and mouse peripheral blood leukocytes (black dots) 1 week after treatment. (**D**) Median survival time ± SD; *p<0.001 and **p<0.002 in comparison to DA.

FLT3 inhibitor downregulated HR and D-NHEJ proteins and inhibited HR and D-NHEJ activity

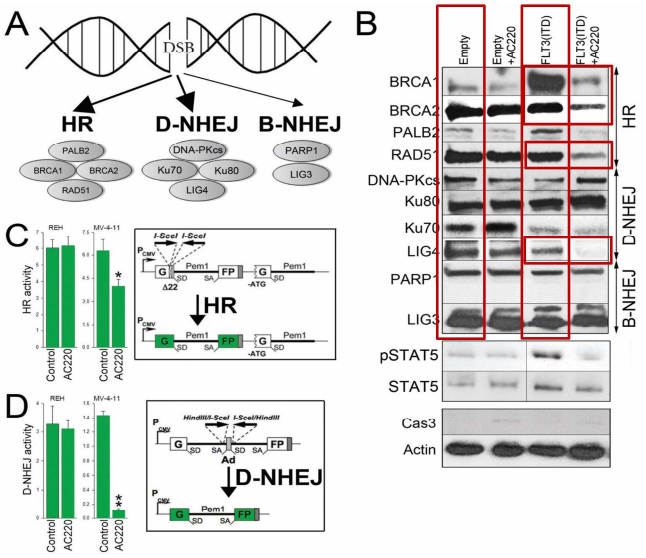

Blood, 2018

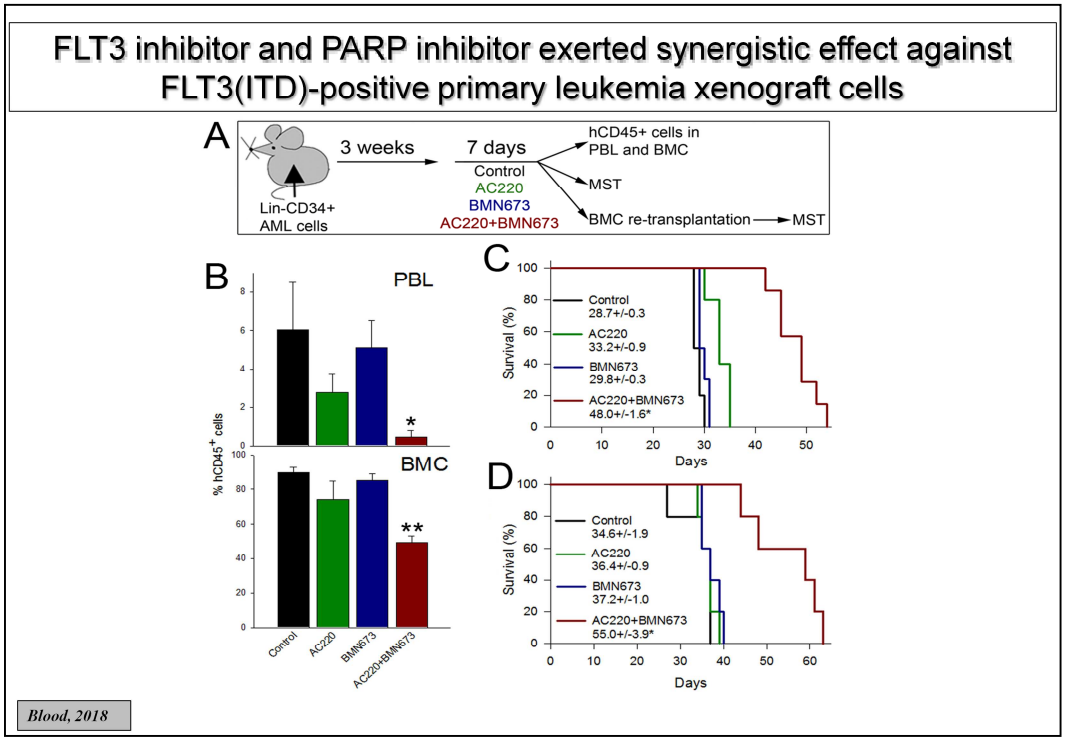

PARP1 inhibitors exerted therapeutic effect against BRCA and/or DNA-PK –deficient positive AML and ALL primary leukemia xenografts. (**A**) Microarray detection of mRNA for the indicated genes in primary AMLs (top graph) and ALLs (middle and bottom graphs) xenografts. Each circle represents individual patient: blue, gray and red circles indicate lower than average, average and higher than average expression levels in BRCA/DNA-PK -deficient AML (top graph), BRCA-deficient ALL (middle graph) and BRCA/DNA-PK – proficient ALL (bottom panel) xenograft cells. (**B**) Number of cells from individual primary xenognaft samples treated with DNR, BMN673, and DNR + BMN673; *p<0.05 in comparison to all other groups. (**C**, D) NSG mice (6 mice/group) were injected with 1 x 10^6 primary leukemia xenograft cells and treated with diluents (C), doxorubicin + cytarabine (DA), BMN673, and DA + BMN673. (**C**) Mean ± SD percentage of human $CD45^+$ cells in peripheral blood leukocytes; *p<0.001 in comparison to other groups. Representatives of flow cytometry detecting human $CD45^+$ leukemia cells (red dots) and mouse peripheral blood leukocytes (black dots) 1 week after treatment. (**D**) Median survival time ± SD; *p<0.001 and **p<0.002 in comparison to DA.

blood

Regular Article

MYELOID NEOPLASIA

Tyrosine kinase inhibitor–induced defects in DNA repair sensitize FLT3(ITD)-positive leukemia cells to PARP1 inhibitors

Silvia Maifrede,[1] Margaret Nieborowska-Skorska,[1] Katherine Sullivan-Reed,[1] Yashodhara Dasgupta,[1] Paulina Podszywalow-Bartnicka,[1,2] Bac Viet Le,[1,2] Martyna Solecka,[1] Zhaorui Lian,[3] Elizaveta A. Belyaeva,[4] Alina Nersesyan,[1] Marcin M. Machnicki,[5] Monika Toma,[1,6] Nicolas Chatain,[7] Małgorzata Rydzanicz,[8] Huaqing Zhao,[9] Jaroslav Jelinek,[10] Katarzyna Piwocka,[3] Tomasz Sliwinski,[4] Tomasz Stoklosa,[5] Rafal Ploski,[8] Thomas Fischer,[11] Stephen M. Sykes,[12] Steffen Koschmieder,[7] Lars Bullinger,[13,14] Peter Valent,[15] Mariusz A. Wasik,[4] Jian Huang,[3] and Tomasz Skorski[1]

[1]Department of Microbiology and Immunology, Temple University Lewis Katz School of Medicine, Philadelphia, PA; [2]Laboratory of Cytometry, Nencki Institute of Experimental Biology, Warsaw, Poland; [3]Department of Pathology and Laboratory Medicine, Temple University Lewis Katz School of Medicine, Philadelphia, PA; [4]Department of Pathology and Laboratory Medicine, University of Pennsylvania, Philadelphia, PA; [5]Department of Immunology, The Medical University of Warsaw, Warsaw, Poland; [6]Laboratory of Medical Genetics, Faculty of Biology and Environmental Protection, University of Lodz, Poland; [7]Department of Hematology, Oncology, Hemostaseology, and Stem Cell Transplantation, Faculty of Medicine, RWTH Aachen University, Aachen, Germany; [8]Department of Medical Genetics, The Medical University of Warsaw, Warsaw, Poland; [9]Department of Clinical Sciences and [10]Fels Institute for Cancer Research and Molecular Biology, Temple University Lewis Katz School of Medicine, Philadelphia, PA; [11]Department of Hematology and Oncology, Center of Internal Medicine, Otto-von-Guericke University Magdeburg, Magdeburg, Germany; [12]Research Institute of Fox Chase Cancer Center, Immune Cell Development and Host Defense, Philadelphia, PA; [13]Department of Internal Medicine III, University of Ulm, Ulm, Germany; [14]Department of Hematology, Oncology and Tumor Immunology, Campus Virchow Klinikum, Charité-University Medicine, Berlin, Germany; and [15]Department of Internal Medicine I, Division of Hematology and Hemostaseology and Ludwig-Boltzmann Cluster Oncology, Medical University of Vienna, Vienna, Austria

KEY POINTS

- FLT3 inhibitor AC220 caused DNA repair defects and sensitized FLT3(ITD)-positive AML stem and progenitor cells to PARP1 inhibitors.
- Quiescent and proliferating FLT3(ITD)-positive AML cells were eliminated by the combination of FLT3 and PARP1 inhibitors.

Mutations in FMS-like tyrosine kinase 3 (FLT3), such as internal tandem duplications (ITDs), can be found in up to 23% of patients with acute myeloid leukemia (AML) and confer a poor prognosis. Current treatment options for FLT3(ITD)-positive AMLs include genotoxic therapy and FLT3 inhibitors (FLT3i's), which are rarely curative. PARP1 inhibitors (PARP1i's) have been successfully applied to induce synthetic lethality in tumors harboring BRCA1/2 mutations and displaying homologous recombination (HR) deficiency. We show here that inhibition of FLT3(ITD) activity by the FLT3i AC220 caused downregulation of DNA repair proteins BRCA1, BRCA2, PALB2, RAD51, and LIG4, resulting in inhibition of 2 major DNA double-strand break (DSB) repair pathways, HR, and nonhomologous end-joining. PARP1i, olaparib, and BMN673 caused accumulation of lethal DSBs and cell death in AC220-treated FLT3(ITD)-positive leukemia cells, thus mimicking synthetic lethality. Moreover, the combination of FLT3i and PARP1i eliminated FLT3(ITD)-positive quiescent and proliferating leukemia stem cells, as well as leukemic progenitors, from human and mouse leukemia samples. Notably, the combination of AC220 and BMN673 significantly delayed disease onset and effectively reduced leukemia-initiating cells in an FLT3(ITD)-positive primary AML xenograft mouse model. In conclusion, we postulate that FLT3i-induced deficiencies in DSB repair pathways sensitize FLT3(ITD)-positive AML cells to synthetic lethality triggered by PARP1i's. Therefore, FLT3(ITD) could be used as a precision medicine marker for identifying AML patients that may benefit from a therapeutic regimen combining FLT3 and PARP1i's. (*Blood*. 2018;132(1):67-77)

PARP1 inhibitors exerted therapeutic effect against BRCA and/or DNA-PK –deficient positive AML and ALL primary leukemia xenografts. (**A**) Microarray detection of mRNA for the indicated genes in primary AMLs (top graph) and ALLs (middle and bottom graphs) xenografts. Each circle represents individual patient: blue, gray and red circles indicate lower than average, average and higher than average expression levels in BRCA/DNA-PK -deficient AML (top graph), BRCA-deficient ALL (middle graph) and BRCA/DNA-PK – proficient ALL (bottom panel) xenograft cells. (**B**) Number of cells from individual primary xenognaft samples treated with DNR, BMN673, and DNR + BMN673; *$p<0.05$ in comparison to all other groups. (**C**, D) NSG mice (6 mice/group) were injected with 1 x 10^6 primary leukemia xenograft cells and treated with diluents (C), doxorubicin + cytarabine (DA), BMN673, and DA + BMN673. (**C**) Mean ± SD percentage of human $CD45^+$ cells in peripheral blood leukocytes; *$p<0.001$ in comparison to other groups. Representatives of flow cytometry detecting human $CD45^+$ leukemia cells (red dots) and mouse peripheral blood leukocytes (black dots) 1 week after treatment. (**D**) Median survival time ± SD; *$p<0.001$ and **$p<0.002$ in comparison to DA.

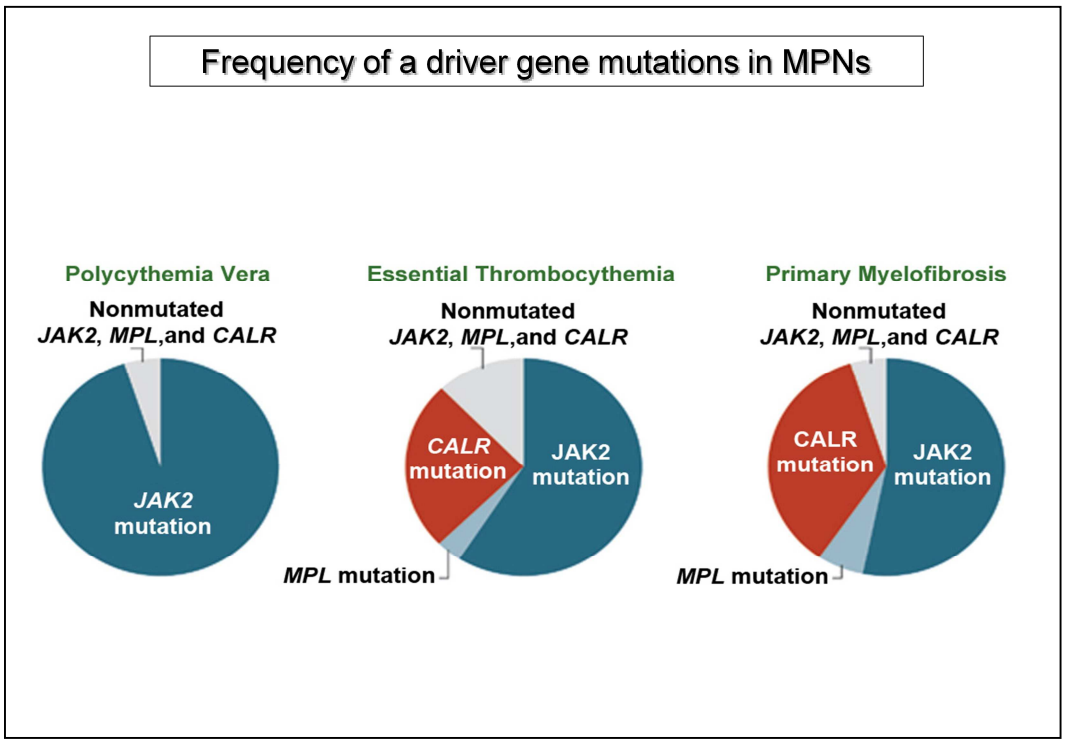

PARP1 inhibitors exerted therapeutic effect against BRCA and/or DNA-PK –deficient positive AML and ALL primary leukemia xenografts. (**A**) Microarray detection of mRNA for the indicated genes in primary AMLs (top graph) and ALLs (middle and bottom graphs) xenografts. Each circle represents individual patient: blue, gray and red circles indicate lower than average, average and higher than average expression levels in BRCA/DNA-PK -deficient AML (top graph), BRCA-deficient ALL (middle graph) and BRCA/DNA-PK – proficient ALL (bottom panel) xenograft cells. (**B**) Number of cells from individual primary xenognaft samples treated with DNR, BMN673, and DNR + BMN673; *$p<0.05$ in comparison to all other groups. (**C**, D) NSG mice (6 mice/group) were injected with 1 x 10^6 primary leukemia xenograft cells and treated with diluents (C), doxorubicin + cytarabine (DA), BMN673, and DA + BMN673. (**C**) Mean ± SD percentage of human $CD45^+$ cells in peripheral blood leukocytes; *$p<0.001$ in comparison to other groups. Representatives of flow cytometry detecting human $CD45^+$ leukemia cells (red dots) and mouse peripheral blood leukocytes (black dots) 1 week after treatment. (**D**) Median survival time ± SD; *$p<0.001$ and **$p<0.002$ in comparison to DA.

JAK1/2 kinase inhibitor downregulated HR and D-NHEJ proteins and inhibited HR and D-NHEJ

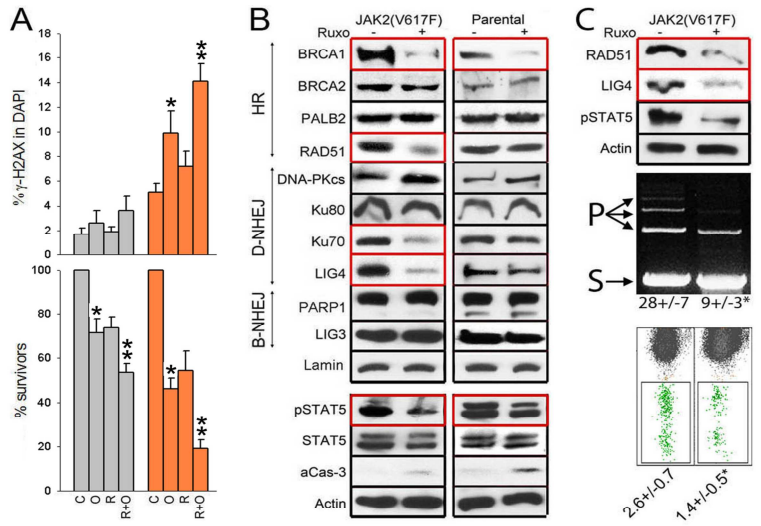

Blood, 2017

BMN673 exerted anti-MPN effect in vivo.

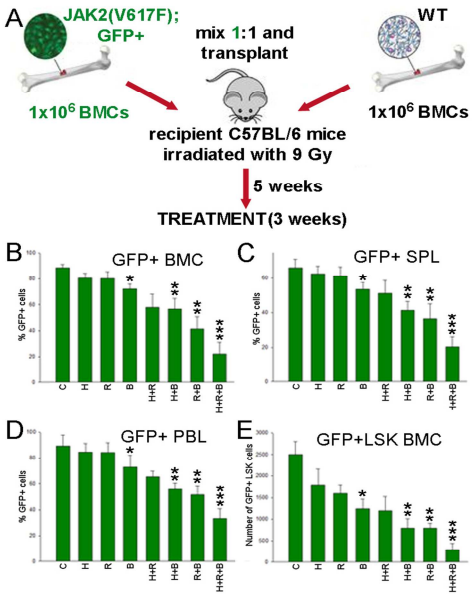

Blood, 2017

Regular Article

blood

MYELOID NEOPLASIA

Ruxolitinib-induced defects in DNA repair cause sensitivity to PARP inhibitors in myeloproliferative neoplasms

Margaret Nieborowska-Skorska,[1] Silvia Maifrede,[1] Yashodhara Dasgupta,[1] Katherine Sullivan,[1] Sylwia Flis,[1,2] Bac Viet Le,[1,3] Martyna Solecka,[1] Elizaveta A. Belyaeva,[4] Lucia Kubovcakova,[5] Morgan Nawrocki,[1] Martin Kirschner,[6] Huaqing Zhao,[7] Josef T. Prchal,[8] Katarzyna Piwocka,[3] Alison R. Moliterno,[9] Mariusz Wasik,[4] Steffen Koschmieder,[6] Tony R. Green,[10-12] Hadek C. Skoda,[5] and Tomasz Skorski[1,13]

[1]Department of Microbiology and Immunology, Lewis Katz School of Medicine, Temple University, Philadelphia, PA; [2]Department of Pharmacology, National Medicines Institute, Warsaw, Poland; [3]Laboratory of Cytometry, Nencki Institute of Experimental Biology, Warsaw, Poland; [4]Department of Pathology and Laboratory Medicine, University of Pennsylvania, Philadelphia, PA; [5]Department of Biomedicine, University Hospital Basel/University of Basel, Basel, Switzerland; [6]Department of Hematology, Oncology, Hemostaseology and Stem Cell Transplantation, Faculty of Medicine, Rheinisch-Westfälische Technische Hochschule Aachen University, Aachen, Germany; [7]Department of Clinical Sciences, Lewis Katz School of Medicine, Temple University, Philadelphia, PA; [8]School of Medicine, University of Utah, Salt Lake City, UT; [9]Division of Hematology, Department of Medicine, School of Medicine, The Johns Hopkins University, Baltimore, MD; and [10]Cambridge Institute for Medical Research, [11]Wellcome–Medical Research Council Cambridge Stem Cell Institute, and [12]Department of Haematology, University of Cambridge, Cambridge, United Kingdom; and [13]Fels Institute for Cancer Research and Molecular Biology, Lewis Katz School of Medicine, Temple University, Philadelphia, PA

Key Points

- Ruxolitinib caused DNA repair defects and sensitized MPN stem and progenitor cells to PARP inhibitors.
- Quiescent and proliferating MPN cells were eliminated by ruxolitinib and olaparib plus or minus hydroxyurea.

Myeloproliferative neoplasms (MPNs) often carry JAK2(V617F), MPL(W515L), or CALR (del52) mutations. Current treatment options for MPNs include cytoreduction by hydroxyurea and JAK1/2 inhibition by ruxolitinib, both of which are not curative. We show here that cell lines expressing JAK2(V617F), MPL(W515L), or CALR(del52) accumulated reactive oxygen species–induced DNA double-strand breaks (DSBs) and were modestly sensitive to poly-ADP-ribose polymerase (PARP) inhibitors olaparib and BMN673. At the same time, primary MPN cell samples from individual patients displayed a high degree of variability in sensitivity to these drugs. Ruxolitinib inhibited 2 major DSB repair mechanisms, BRCA-mediated homologous recombination and DNA-dependent protein kinase–mediated nonhomologous end-joining, and, when combined with olaparib, caused abundant accumulation of toxic DSBs resulting in enhanced elimination of MPN primary cells, including the disease-initiating cells from the majority of patients. Moreover, the combination of BMN673, ruxolitinib, and hydroxyurea was highly effective in vivo against JAK2(V617F)$^+$ murine MPN-like disease and also against JAK2(V617F)$^+$, CALR(del52)$^+$, and MPL(W515L)$^+$ primary MPN xenografts. In conclusion, we postulate that ruxolitinib-induced deficiencies in DSB repair pathways sensitized MPN cells to synthetic lethality triggered by PARP inhibitors. (*Blood*. 2017;130(26):2848-2859)

Personalized medicine-guided synthetic lethality in MPNs

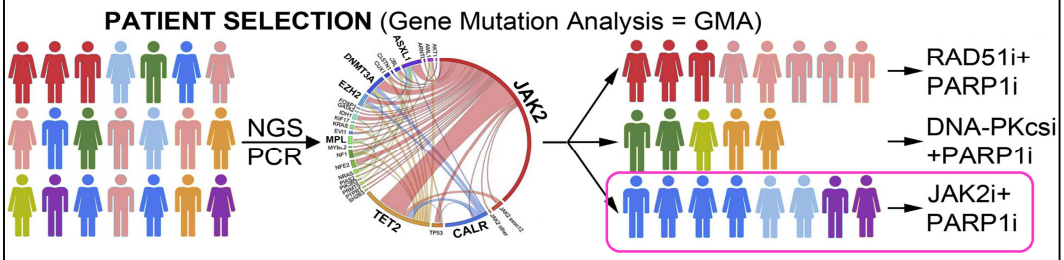

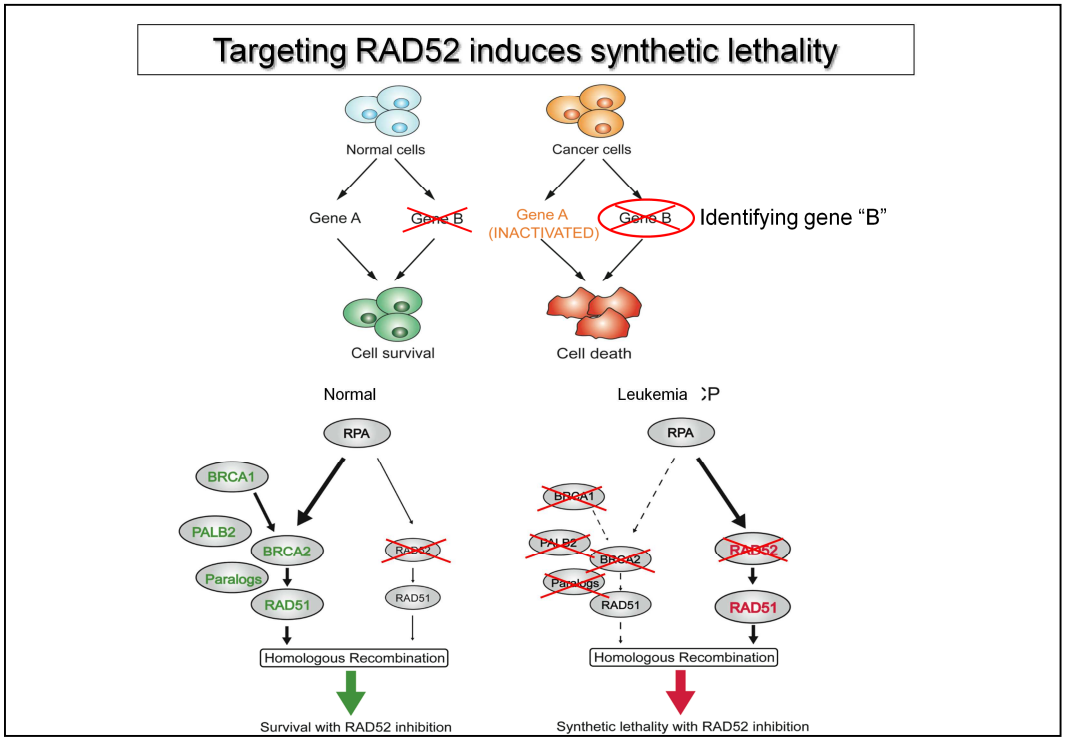

Given BCR-ABLs wide influence on many cellualr pathways, identification of a so-called gene B is difficult, however since CML cells have so many double strand breaks we focused on the recombination pathway. In normal cells, the left arm of this pathway is used involving BRCA1/2 with the RAD52 pathway used only as a backup which was confirmed by immunofluorescence. In CML cells however, the BRCA1 protein is downregulated by BCR-ABL leaving these cells to be heavily reliant on RAD52 for double-strand break repair. This was also confirmed by immunofluorescence studies.

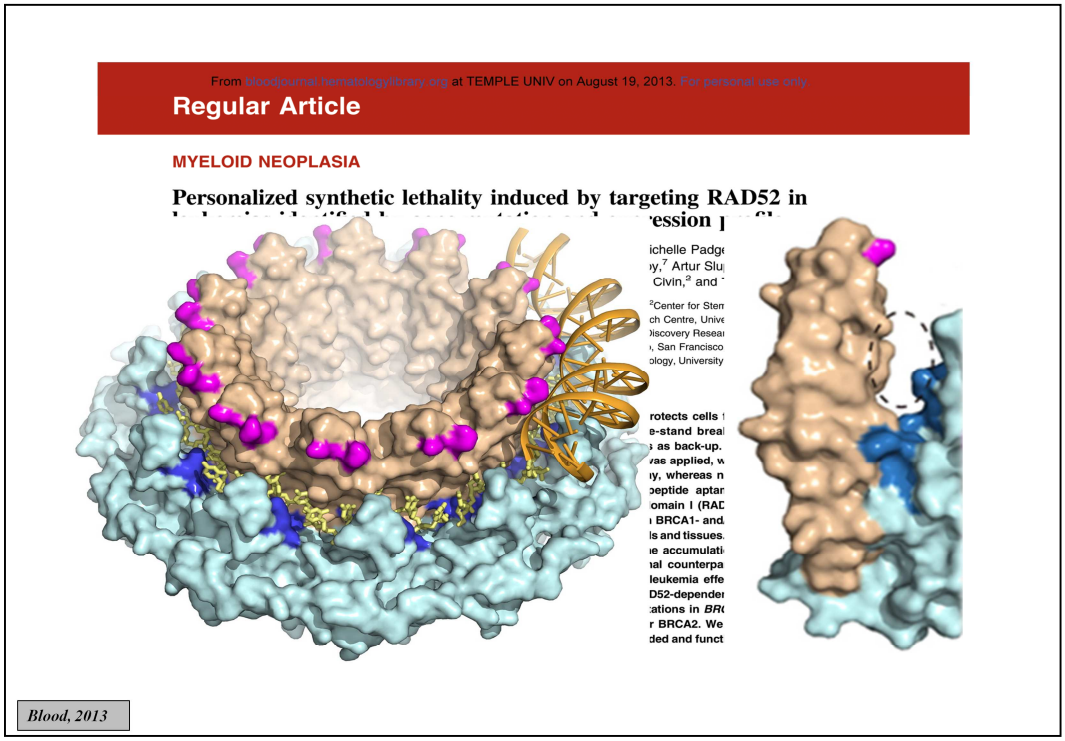

PARP1 inhibitors exerted therapeutic effect against BRCA and/or DNA-PK –deficient positive AML and ALL primary leukemia xenografts. (**A**) Microarray detection of mRNA for the indicated genes in primary AMLs (top graph) and ALLs (middle and bottom graphs) xenografts. Each circle represents individual patient: blue, gray and red circles indicate lower than average, average and higher than average expression levels in BRCA/DNA-PK -deficient AML (top graph), BRCA-deficient ALL (middle graph) and BRCA/DNA-PK – proficient ALL (bottom panel) xenograft cells. (**B**) Number of cells from individual primary xenognaft samples treated with DNR, BMN673, and DNR + BMN673; *p<0.05 in comparison to all other groups. (**C**, D) NSG mice (6 mice/group) were injected with 1 x 10^6 primary leukemia xenograft cells and treated with diluents (C), doxorubicin + cytarabine (DA), BMN673, and DA + BMN673. (**C**) Mean ± SD percentage of human $CD45^+$ cells in peripheral blood leukocytes; *p<0.001 in comparison to other groups. Representatives of flow cytometry detecting human $CD45^+$ leukemia cells (red dots) and mouse peripheral blood leukocytes (black dots) 1 week after treatment. (**D**) Median survival time ± SD; *p<0.001 and **p<0.002 in comparison to DA.

Development of RAD52 small molecule inhibitor

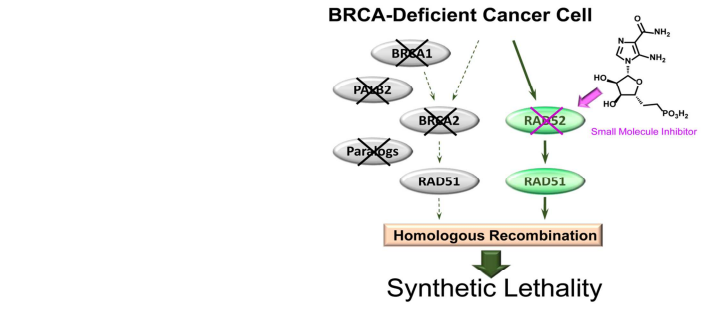

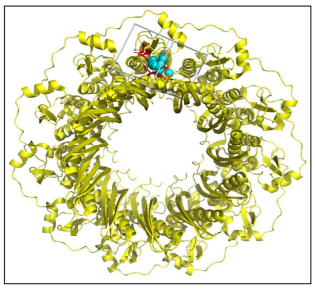

Skorski &Hromas

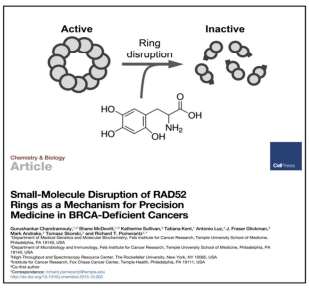

Pomerantz & Skorski

Mazin & Skorski

Since there are currently no published Rad52 inhibitors, we along with two of our collaborators have independently conducted large scale screens for candidate RAD52 inhibitors that have resulted in a total of three candidate Rad52 inhibitors that all target Rad52 via a different mode of action

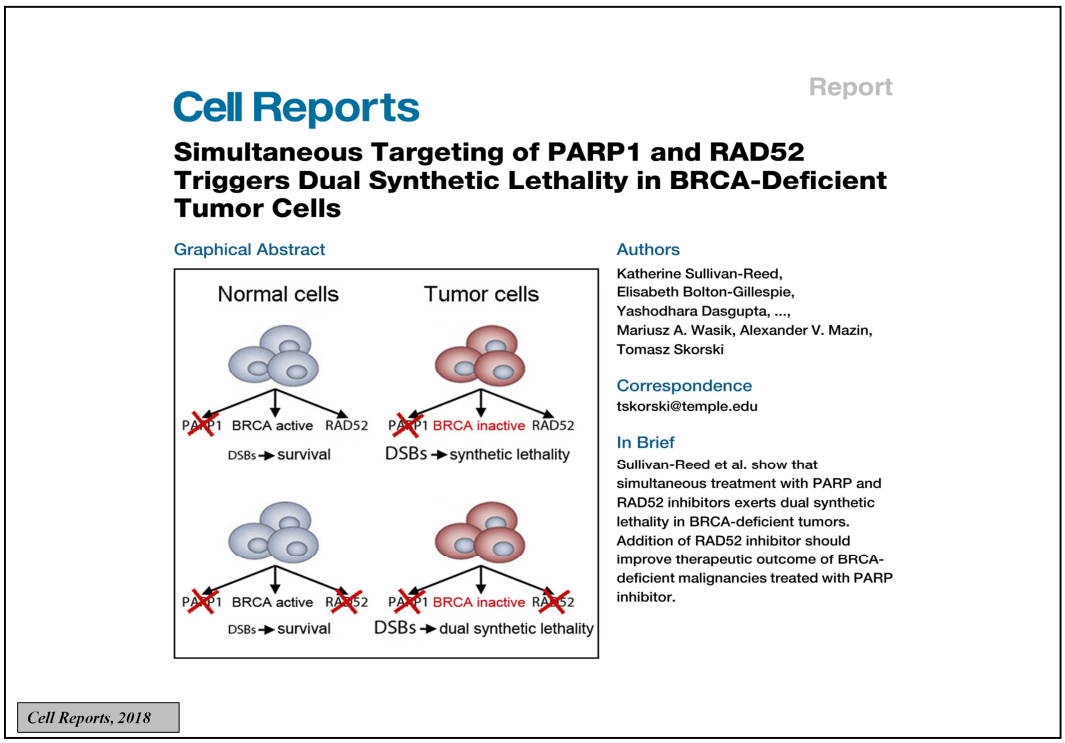

Report

Cell Reports

Simultaneous Targeting of PARP1 and RAD52 Triggers Dual Synthetic Lethality in BRCA-Deficient Tumor Cells

Graphical Abstract

Authors

Katherine Sullivan-Reed, Elisabeth Bolton-Gillespie, Yashodhara Dasgupta, ..., Mariusz A. Wasik, Alexander V. Mazin, Tomasz Skorski

Correspondence

tskorski@temple.edu

In Brief

Sullivan-Reed et al. show that simultaneous treatment with PARP and RAD52 inhibitors exerts dual synthetic lethality in BRCA-deficient tumors. Addition of RAD52 inhibitor should improve therapeutic outcome of BRCA-deficient malignancies treated with PARP inhibitor.

Cell Reports, 2018

PARP1 inhibitors exerted therapeutic effect against BRCA and/or DNA-PK –deficient positive AML and ALL primary leukemia xenografts. (**A**) Microarray detection of mRNA for the indicated genes in primary AMLs (top graph) and ALLs (middle and bottom graphs) xenografts. Each circle represents individual patient: blue, gray and red circles indicate lower than average, average and higher than average expression levels in BRCA/DNA-PK -deficient AML (top graph), BRCA-deficient ALL (middle graph) and BRCA/DNA-PK – proficient ALL (bottom panel) xenograft cells. (**B**) Number of cells from individual primary xenognaft samples treated with DNR, BMN673, and DNR + BMN673; *$p<0.05$ in comparison to all other groups. (**C**, D) NSG mice (6 mice/group) were injected with 1 x 10^6 primary leukemia xenograft cells and treated with diluents (C), doxorubicin + cytarabine (DA), BMN673, and DA + BMN673. (**C**) Mean ± SD percentage of human $CD45^+$ cells in peripheral blood leukocytes; *$p<0.001$ in comparison to other groups. Representatives of flow cytometry detecting human $CD45^+$ leukemia cells (red dots) and mouse peripheral blood leukocytes (black dots) 1 week after treatment. (**D**) Median survival time ± SD; *$p<0.001$ and **$p<0.002$ in comparison to DA.

Simultaneous targeting of RAD52 and PARP by small molecule inhibitors eradicated BRCA-deficient cells

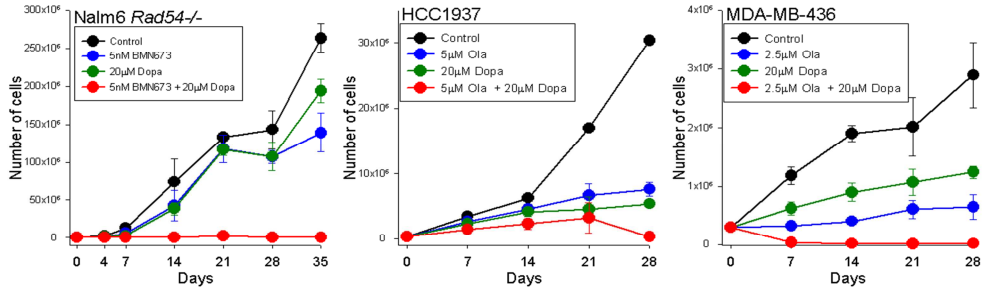

PARP1 inhibitors exerted therapeutic effect against BRCA and/or DNA-PK –deficient positive AML and ALL primary leukemia xenografts. (**A**) Microarray detection of mRNA for the indicated genes in primary AMLs (top graph) and ALLs (middle and bottom graphs) xenografts. Each circle represents individual patient: blue, gray and red circles indicate lower than average, average and higher than average expression levels in BRCA/DNA-PK -deficient AML (top graph), BRCA-deficient ALL (middle graph) and BRCA/DNA-PK – proficient ALL (bottom panel) xenograft cells. (**B**) Number of cells from individual primary xenognaft samples treated with DNR, BMN673, and DNR + BMN673; *p<0.05 in comparison to all other groups. (**C**, D) NSG mice (6 mice/group) were injected with 1 x 10^6 primary leukemia xenograft cells and treated with diluents (C), doxorubicin + cytarabine (DA), BMN673, and DA + BMN673. (**C**) Mean ± SD percentage of human $CD45^+$ cells in peripheral blood leukocytes; *p<0.001 in comparison to other groups. Representatives of flow cytometry detecting human $CD45^+$ leukemia cells (red dots) and mouse peripheral blood leukocytes (black dots) 1 week after treatment. (**D**) Median survival time ± SD; *p<0.001 and **p<0.002 in comparison to DA.

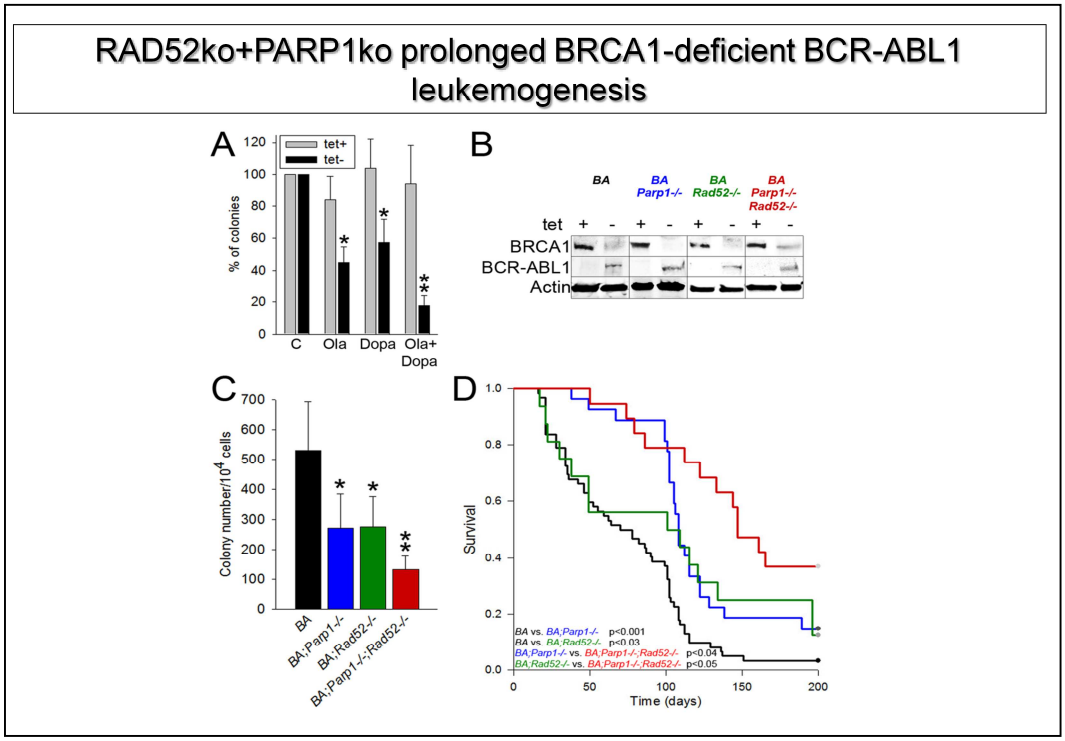

PARP1 inhibitors exerted therapeutic effect against BRCA and/or DNA-PK –deficient positive AML and ALL primary leukemia xenografts. (**A**) Microarray detection of mRNA for the indicated genes in primary AMLs (top graph) and ALLs (middle and bottom graphs) xenografts. Each circle represents individual patient: blue, gray and red circles indicate lower than average, average and higher than average expression levels in BRCA/DNA-PK -deficient AML (top graph), BRCA-deficient ALL (middle graph) and BRCA/DNA-PK – proficient ALL (bottom panel) xenograft cells. (**B**) Number of cells from individual primary xenognaft samples treated with DNR, BMN673, and DNR + BMN673; *p<0.05 in comparison to all other groups. (**C**, D) NSG mice (6 mice/group) were injected with 1 x 10^6 primary leukemia xenograft cells and treated with diluents (C), doxorubicin + cytarabine (DA), BMN673, and DA + BMN673. (**C**) Mean ± SD percentage of human $CD45^+$ cells in peripheral blood leukocytes; *p<0.001 in comparison to other groups. Representatives of flow cytometry detecting human $CD45^+$ leukemia cells (red dots) and mouse peripheral blood leukocytes (black dots) 1 week after treatment. (**D**) Median survival time ± SD; *p<0.001 and **p<0.002 in comparison to DA.

Simultaneous targeting of RAD52 and PARP in mice bearing BRCA-deficient human tumor cells

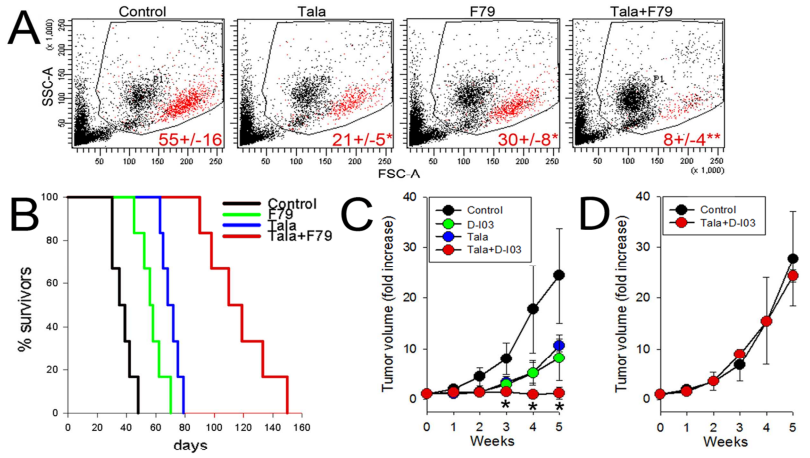

PARP1 inhibitors exerted therapeutic effect against BRCA and/or DNA-PK –deficient positive AML and ALL primary leukemia xenografts. (**A**) Microarray detection of mRNA for the indicated genes in primary AMLs (top graph) and ALLs (middle and bottom graphs) xenografts. Each circle represents individual patient: blue, gray and red circles indicate lower than average, average and higher than average expression levels in BRCA/DNA-PK -deficient AML (top graph), BRCA-deficient ALL (middle graph) and BRCA/DNA-PK – proficient ALL (bottom panel) xenograft cells. (**B**) Number of cells from individual primary xenognaft samples treated with DNR, BMN673, and DNR + BMN673; *p<0.05 in comparison to all other groups. (**C**, D) NSG mice (6 mice/group) were injected with 1 x 10^6 primary leukemia xenograft cells and treated with diluents (C), doxorubicin + cytarabine (DA), BMN673, and DA + BMN673. (**C**) Mean ± SD percentage of human $CD45^+$ cells in peripheral blood leukocytes; *p<0.001 in comparison to other groups. Representatives of flow cytometry detecting human $CD45^+$ leukemia cells (red dots) and mouse peripheral blood leukocytes (black dots) 1 week after treatment. (**D**) Median survival time ± SD; *p<0.001 and **p<0.002 in comparison to DA.

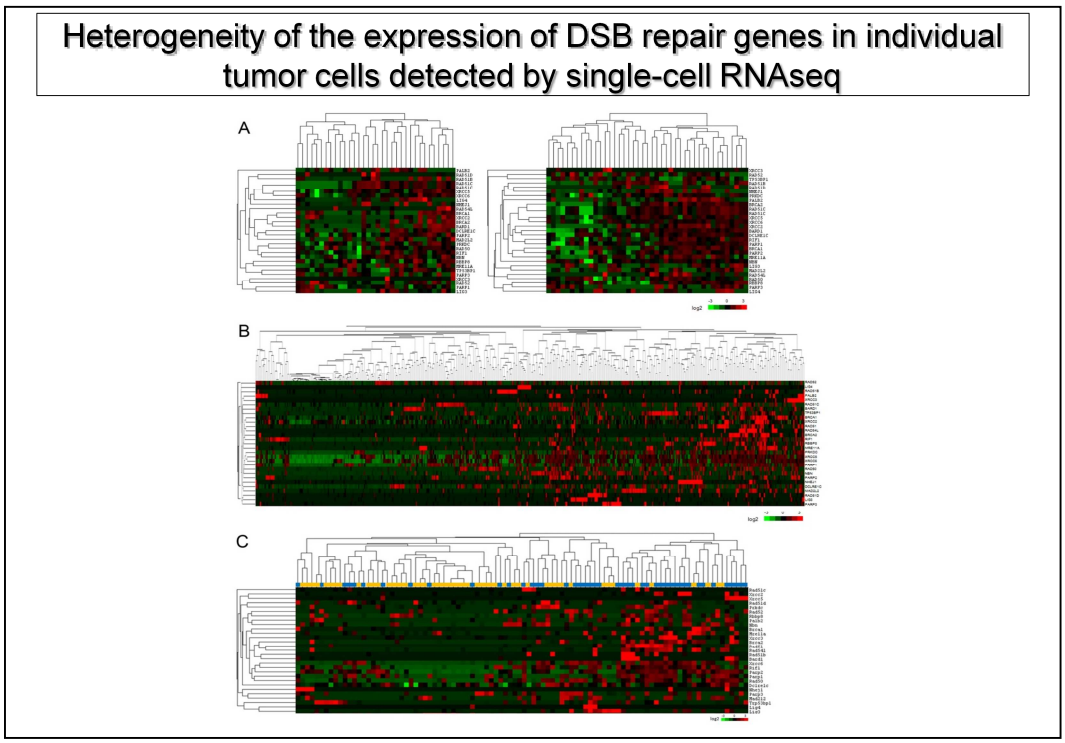

qRT-PCR identifies individual patients with BRCA-deficient and DNA-PK-deficient ALLs which are sensitive to BMN673. (**A**) qRT-PCR analysis of the expression of DSB repair genes in 9 primary ALL xenografts. BRCA-deficient and/or DNA-PK-deficient (>2-fold downregulation in comparison to mean expression level for at least one gene in BRCA and/or DNA-PK pathways; blue bars) and BRCA-proficient/DNA-PK-proficient (red bars) samples; samples used in further analyses are marked by asterisks. (**B**) Number of primary ALL xenograft cells from individual BRCA-deficient and/or DNA-PK-deficient (blue bars) and BRCA-proficient/DNA-PK-proficient (red bars) samples treated with DNR, BMN673, and DNR + BMN673. (**C**) Cumulative mean percentage ± SD of the results from samples examined in section **B**; *$p<0.02$ and **$p=0.002$.

Acknowledgements

Tomasz Skorski's Lab
Temple University School of Medicine
-Margaret Nieborowska-Skorska
-Kimberly Cramer-Morales
-Artur Slupianek
-Elisabeth Bolton-Gillespie
-Katherine Sullivan
-Silvia Maifrede

Mark Minden's lab
University of Toronto

Kolja Eppert's lab
McGill University, Montreal

Markus Müschen's lab
University of California San Francisco
-Jaewoong Lee

Katarzyna Piwocka's lab
Nencki Institute of Experimental Biology, Warsaw, Poland
-Paulina Podszywalow-Bartnicka

Italo Tempera's lab
Temple University School of Medicine

Curt Civin's lab
University of Maryland, Baltimore, MD

Peter Valent and Sabine Cerny-Reiterer
Medical University of Vienna

Stephen Sykes's lab
Fox Chase Cancer Center, Philadelphia, PA
-Chun Zhou

Grazyna Hoser
Medical Center of Postgraduate Education, Poland

Tomasz Stoklosa
Medical University of Warsaw, Poland

Richard Pomerantz
Temple University School of Medicine

Alexander Mazin
Drexel University

Funding:
NIH/NCI, LLS, WES, SPORE from MDAnderson Cancer Center

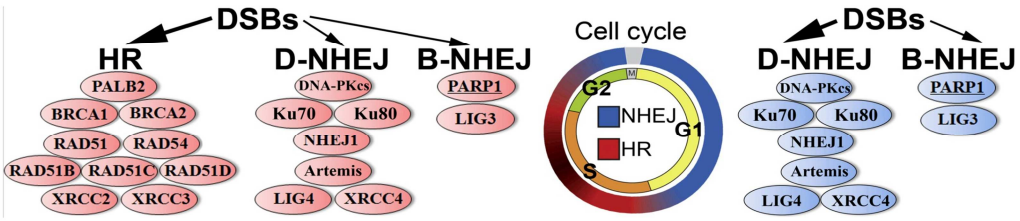
DSBs
HR
D-NHEJ
B-NHEJ
PALB2
BRCA1
BRCA2
RAD51
RAD54
RAD51B
RAD51C
RAD51D
XRCC2
XRCC3
DNA-PKcs
Ku70
Ku80
NHEJ1
Artemis
LIG4
XRCC4
PARP1
LIG3
Cell cycle
G2
M
NHEJ
HR
G1
S
DSBs
D-NHEJ
B-NHEJ
DNA-PKcs
Ku70
Ku80
NHEJ1
Artemis
LIG4
XRCC4
PARP1
LIG3

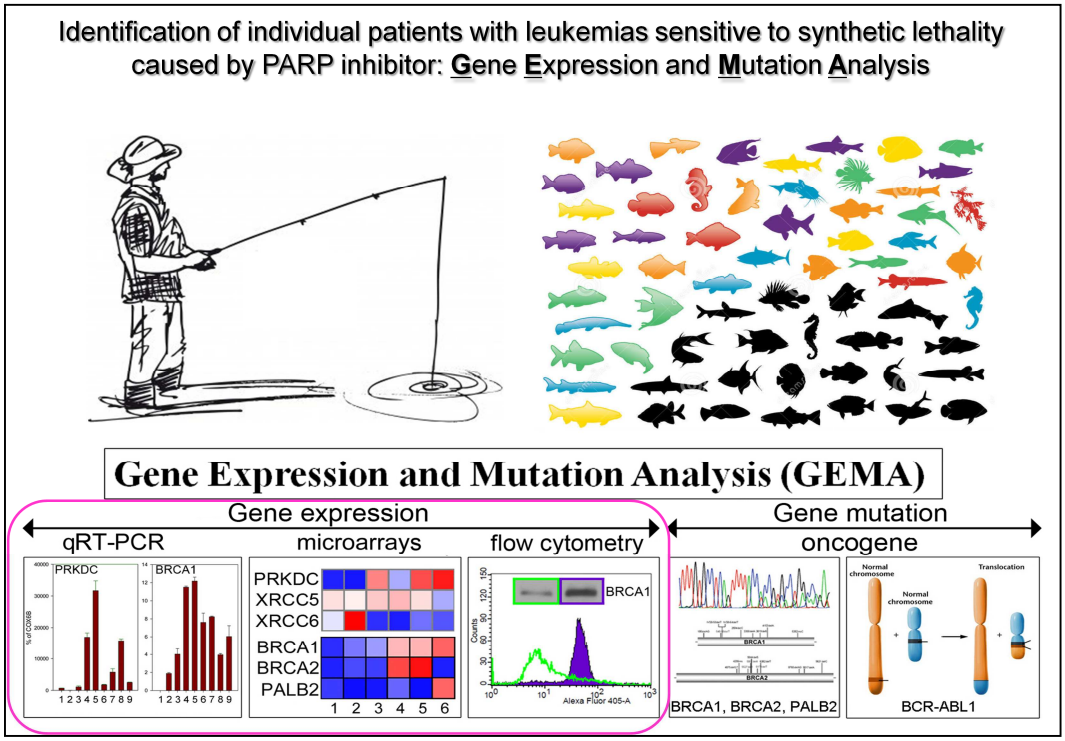

GEMA to select "BRCA-deficient" AML/ALL patients. Gene expression analysis by quantization of the expression patterns of BRCA-pathway genes by qRT-PCR, mRNA microarrays and flow cytometry. Mutation analysis by detection of particular genetic aberration (mutation, chromosomal translocation).

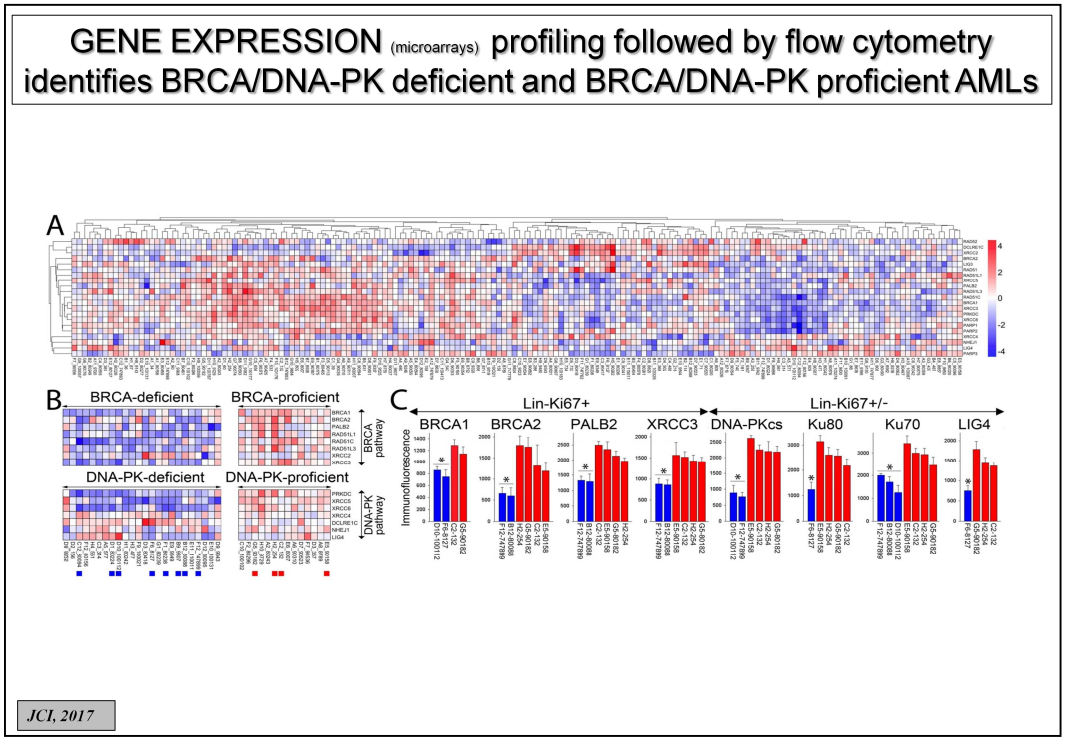

Microarrays identify individual patients with BRCA-deficient and DNA-PK-deficient AMLs which are sensitive to BMN673. (**A**) Microarray analysis of the expression of DSB repair genes in 186 AML patients. (**B**) BRCA-deficient/DNA-PK-deficient (row Z-score <-1.5 for at least one gene in BRCA and DNA-PK pathways) and BRCA-proficient/DNA-PK-proficient (row Z-score >-.075 for all genes in BRCA and DNA-PK pathways) samples; samples used in further analyses are marked by asterisks. (**C**) Flow cytometry analysis of the indicated DSB repair proteins in AMLs from individual patients; *p<0.05 in comparison to BRCA-proficient/DNA-PK-proficient cells. (**D**) DSBs detected by g-H2AX immunofluorescence in untreated controls and in BRCA-deficient/DNA-PK-deficient (blue) and BRCA-proficient/DNA-PK-proficient (red) cells treated with daunorubicin (DNR), BMN673, and DNR + BMN673; *p<0.05 in comparison to DNR. (**E**) Survival of Lin^- AML cells from BRCA-deficient/DNA-PK-deficient (blue, n=9) and BRCA-proficient/DNA-PK-proficient (red, n-4) samples treated with BMN673 (left panel) and DNR + BMN673 (right panel). (**F**) Number of proliferating Lin-CD38-CTV^{low} and quiescent Lin-CD38-CTV^{max} cells from individual BRCA-deficient/DNA-PK-deficient (blue) and BRCA-proficient/DNA-PK-proficient (red) samples treated with DNR, BMN673, and DNR + BMN673. (**G**) Cumulative mean percentage ± SD of the results from samples examined in previous section; *p<0.02 and **p<0.05.

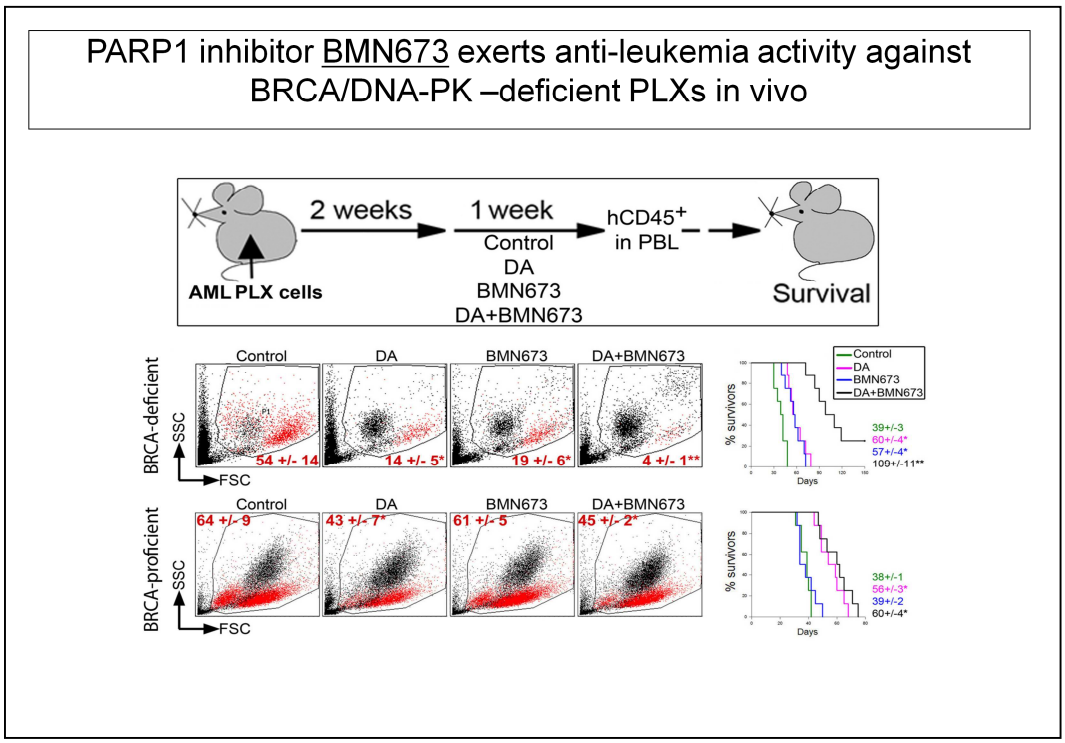

PARP1 inhibitors exerted therapeutic effect against BRCA and/or DNA-PK –deficient positive AML and ALL primary leukemia xenografts. (**A**) Microarray detection of mRNA for the indicated genes in primary AMLs (top graph) and ALLs (middle and bottom graphs) xenografts. Each circle represents individual patient: blue, gray and red circles indicate lower than average, average and higher than average expression levels in BRCA/DNA-PK -deficient AML (top graph), BRCA-deficient ALL (middle graph) and BRCA/DNA-PK – proficient ALL (bottom panel) xenograft cells. (**B**) Number of cells from individual primary xenognaft samples treated with DNR, BMN673, and DNR + BMN673; *p<0.05 in comparison to all other groups. (**C**, D) NSG mice (6 mice/group) were injected with 1 x 10^6 primary leukemia xenograft cells and treated with diluents (C), doxorubicin + cytarabine (DA), BMN673, and DA + BMN673. (**C**) Mean ± SD percentage of human $CD45^+$ cells in peripheral blood leukocytes; *p<0.001 in comparison to other groups. Representatives of flow cytometry detecting human $CD45^+$ leukemia cells (red dots) and mouse peripheral blood leukocytes (black dots) 1 week after treatment. (**D**) Median survival time ± SD; *p<0.001 and **p<0.002 in comparison to DA.